European Journal of Radiology Open 2 (2015) 101–110

Contents lists available at ScienceDirect

European Journal of Radiology Open

journal homepage: www.elsevier.com/locate/ejro

Review article

CT and MR imaging findings of systemic complications occurring during pregnancy and puerperal period, adversely affected by natural changes

Yuki Himoto[a,1], Aki Kido[a,*], Yusaku Moribata[a,1], Toshihide Yamaoka[b], Ryosuke Okumura[c], Kaori Togashi[a,1]

[a] Department of Diagnostic Imaging and Nuclear Medicine, Graduate School of Medicine, Kyoto University, 54 Shogoinkawahara-cho, Sakyo-ku, Kyoto 606-8507, Japan
[b] Department of Radiology, Kyoto Katsura Hospital, 17 Yamada Hirao-cho, Nishikyo-ku, Kyoto 615-8256, Japan
[c] Department of Radiology, Kitano Hospital, 2-4-20 Ohgimachi, Kita-ku, Osaka-shi, Osaka-fu 530-8480, Japan

ARTICLE INFO

Article history:
Received 21 April 2015
Accepted 23 May 2015
Available online 15 June 2015

Keywords:
CT
MR
Pregnancy
Non-obstetric complications

ABSTRACT

Dynamic physiological and anatomical changes for delivery may adversely induce various specific non-obstetric complications during pregnancy and puerperal period. These complications can be fatal to both the mother and the fetus, thus a precise and early diagnosis ensued by an early treatment is essential. Along with ultrasonography, computed tomography (CT) and magnetic resonance imaging (MRI) have assumed an increasing role in the diagnosis.

This article aims to discuss the pathophysiology of these complications, the indications for CT and MRI, and the imaging findings.

Contents

* Corresponding author. Tel.: +81 75 751 3760; fax: +81 75 771 9709.
E-mail addresses: yhimoto@kuhp.kyoto-u.ac.jp (Y. Himoto), akikido@kuhp.kyoto-u.ac.jp (A. Kido), moribata@kuhp.kyoto-u.ac.jp (Y. Moribata), to4.yamaok@gmail.com (T. Yamaoka), okumura@kitano-hp.or.jp (R. Okumura), ktogashi@kuhp.kyoto-u.ac.jp (K. Togashi).
[1] Tel.: +81 75 751 3760; fax: +81 75 771 9709.

http://dx.doi.org/10.1016/j.ejro.2015.05.004

1. Introduction

During pregnancy and puerperal period, a dynamic range of physiological and physical changes take place in the woman, to prepare her body for delivery. These changes include coagulation, hemodynamic and hormonal changes, as well as changes in mechanical pressure due to an enlarged uterus. Although these systemic changes are not pathologic, they sometimes lead to various adverse effects. Along with ultrasonography, imaging technologies such as computed tomography (CT) and magnetic resonance imaging (MRI) allow for a precise and prompt diagnosis when these situations occur. It is thus of prime importance for radiologists to understand the pathophysiology underlying these complications, the appropriate imaging modalities to employ, and the associated imaging findings.

In this review, we aim to present the physiological and physical changes taking place in women during pregnancy and puerperal period. In addition, we provide an overview of the non-obstetric complications arising during pregnancy, with a special focus on CT and MRI findings and their roles in diagnosis.

2. Coagulation system

Pregnancy is a state of hypercoagulability, characterized by an increase in fibrinogen and coagulation factors and a decrease of fibrinolytic activity, in preparation for blood loss at delivery. This hypercoagulability, when combined with other pregnancy-associated physiological and physical changes, may lead to venous thromboembolism (VTE) including pulmonary embolism (PE), and in some cases, acute cerebral infarction.

2.1. Venous thromboembolism

Virchow's triad defines the risk factors of VTE as the combination of venous stasis, venous trauma, and hypercoagulability. These conditions arise simultaneously and continuously during pregnancy. The incidence is 0.76–1.72:1000 pregnancies [1]. In comparison to non-pregnant women, the risk of VTE is increased by 5-fold during pregnancy and by 60-fold in the first 3 months after delivery.

Approximately 60–80% of VTEs related to pregnancy are deep venous thrombosis (DVT), the formation of thrombi in large veins. VTE most commonly occurs in the lower limbs, especially in the left flank, likely due to compression by the right iliac artery and the enlarged uterus [1,2]. DVT is reported as the most common cause of PE, a leading cause of maternal mortality in the developed world [2,3]. The risk of PE is increased by 2-fold during pregnancy and by up to 30-fold in the first 3 months after delivery, most frequently in the second week [1]. The D-dimer test cannot be used reliably to exclude PE, as D-dimer levels may be elevated during pregnancy even in the absence of thrombosis. Pulmonary CT angiography or ventilation–perfusion (V/Q) scintigraphy is recommended, when lower extremity Doppler ultrasonography examination fails to detect DVT, despite the clinical suspicion of PE. The mortality associated with untreated PE outweighs by far the risks associated with fetal radiation exposure, thus it is highly recommended to immediately perform CT angiography or V/Q scintigraphy in such cases. On CT angiography, the thrombosis may be visualized as a low-attenuation filling defect of the pulmonary arteries, with or without enlargement (Fig. 1). On V/Q scintigraphy, perfusion defects with ventilation–perfusion mismatch are classically observed. If DVT is found upon US examination, further testing is not necessary because the clinical treatment remains the same [4].

It is important to state that radiation doses may be reduced to a minimum by modifying imaging protocols, but without compromising accuracy [5]. Omitting venography and using lead shielding around the abdomen upon CT angiography, or omitting the ventilation portion in V/Q scintigraphy can help reduce radiation doses [4].

2.2. Ovarian vein thrombosis and septic pelvic thrombophlebitis

Ovarian vein thrombosis (OVT) complicates 0.5–1.8:1000 deliveries, classically during the postpartum period [6]. Typical symptoms are fever, lower abdominal pain, and presence of a lower abdominal mass, representing a thrombosed vein with a surrounding phlegmon. OVT is diagnosed on the right flank in 90% of patient cases. One possible explanation for this right-sided predominance is the retrograde flow from the left ovarian vein and the anterograde flow into the right ovarian vein during the early puerperium, primarily due to the displacement of the uterus to the right by the underlying colon [6].

Septic pelvic thrombophlebitis (SPT) is a clinical condition characterized by inflammation of pelvic veins with infected thrombosis. The incidence is documented at 0.3:1000 deliveries, and occurs

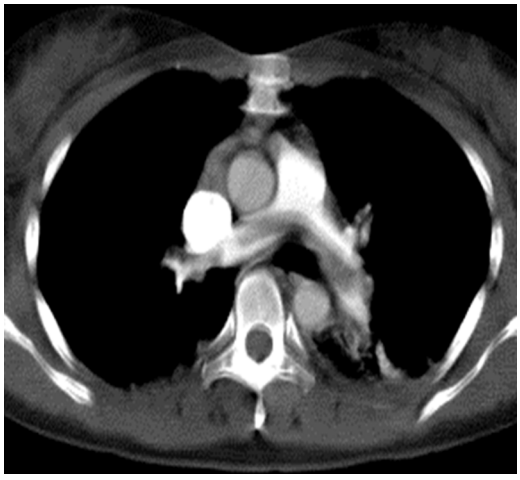

Fig. 1. Characteristic CT scan showing pulmonary embolism in a woman who developed cardiopulmonary arrest 1 day after delivery. Thrombosis crossing the bilateral pulmonary arteries was visualized as a defect on contrast-enhanced CT.

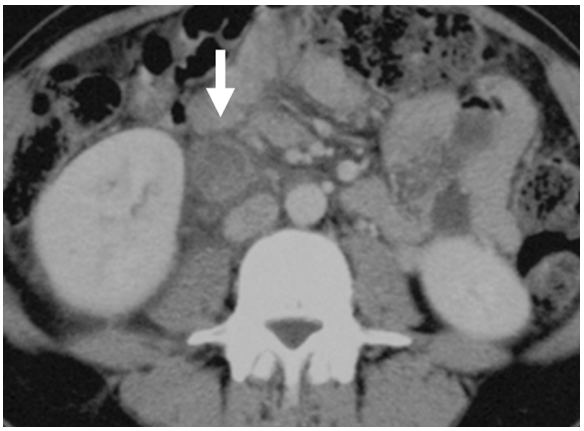

Fig. 2. Characteristic CT scan of septic puerperal ovarian vein thrombosis in a woman presenting high fever after delivery. Thrombosis of the right ovarian vein was depicted as a defect on contrast-enhanced CT (arrow). Inflammation around the vein could also be clearly observed.

more commonly after a cesarean section than a vaginal delivery [7]. Typical symptoms are a high, spiking fever without severe abdominal pain or sepsis. A continuum between SPT and OVT, arising from the conditions described in Virchow's triad, has been suggested [6].

Early recognition is critical because a delayed diagnosis may lead to fatal conditions such as PE and sepsis. Color or power Doppler ultrasonography examination of pelvic veins is the primary imaging modality used, but may not be as sensitive as CT or MRI. Contrast enhanced CT (CECT) venography was reported as the most accurate imaging approach [8]. On CECT, filling defect within the vein, thickening blood vessel wall, and the surrounding inflammatory changes may be observed (Fig. 2) [8]. Unenhanced CT shows characteristic findings such as enlarged vein, thrombus with increased or similar attenuation relative to the wall of the vein. CT is also a useful tool to distinguish these conditions from other complications, such as acute appendicitis [9,10]. Contrast enhanced MR venography, including coronal images, can also be employed to visualize a thrombus and its extension, without the use of radiation [11]. Unenhanced MR venography represents another imaging modality, especially recommended in prepartum patients in whom the use of contrast materials is not recommended [12].

2.3. Ischemic stroke

Stroke is also a leading cause of maternal mortality. Strokes can mimic other more common complications such as eclampsia, therefore, should be considered whenever neurological deterioration is observed. Estimates of incidence of stroke associated with pregnancy vary widely in previous reports. The incidence of non-hemorrhagic and hemorrhagic stroke were reported at 18:100,000 and 8:100,000 pregnancies, respectively [13]. The incidence of fatal stroke is 1.6:100,000 pregnancies [14]. Here, we place the focus on ischemic stroke.

The incidence of ischemic stroke is estimated to increase by 3-fold in pregnant women, possibly explained by the state of relative hypercoagulability [15]. The greatest risk is reported in the 2 days before and the 1 day period after delivery. Cardio-embolism is the most commonly reported etiology. CT and MRI are the major imaging modalities in the diagnosis. CT presents the advantages of availability and rapidness and allows ruling out hemorrhagic stroke, while the major benefits of MRI are its higher sensitivity, especially with diffusion weighted imaging (DWI), and the elimination of radiation exposure (Fig. 3).

In some cases, infarction occurs secondarily to cerebral venous sinus thrombosis (CVST) [13]. The incidence of CVST also increases

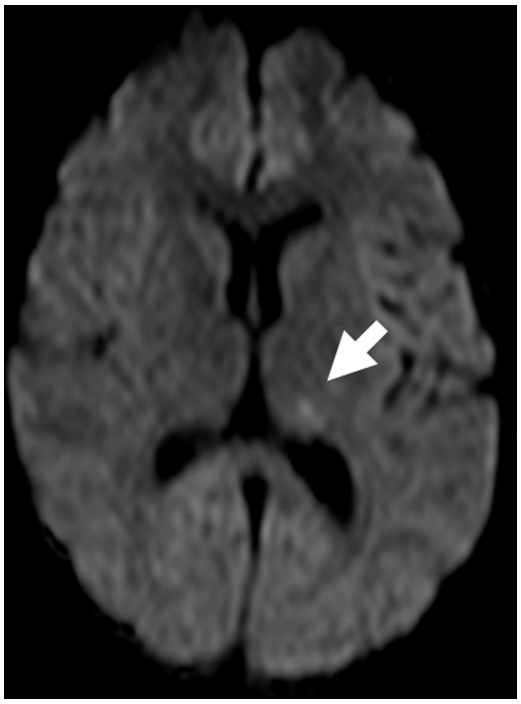

Fig. 3. MRI scan of ischemic infarction in a woman presenting motor weakness in the right arm and leg at 26 gestational weeks. Diffusion-weighted images (DWI) revealed a left thalamic infarction (arrow).

during pregnancy due to hypercoagulability, most significantly in the first 2 weeks of puerperium [16]. CVST should be considered if an edema or a hemorrhagic lesion crossing arterial territories is observed. Both CT and MR venography may be used as accurate imaging modalities, however the latter may be preferred in pregnancy-associated CVST, as it eliminates exposure to ionizing radiation and use of iodinated contrast media [16].

3. Hemodynamic changes

To support the rapidly growing fetus and the placenta, and to safeguard the mother against blood loss associated with delivery, the total blood volume begins to increase during the 1st trimester. Along with an increase in blood volume, there is also a concomitant augmentation in cardiac output and heart rate [17]. Altogether, these hyperdynamic changes may lead to various complications, further discussed below.

3.1. Rupture of brain aneurysm and hemorrhagic stroke

A higher proportion (40%) of hemorrhagic stroke is reported during pregnancy, compared to the non-pregnant population (22%) [18]. A ruptured aneurysm is a common cause of subarachnoid hemorrhage (SAH), while eclampsia or preeclampsia is often associated with intracranial hemorrhage [13,16,18]. It is arguable whether pregnancy is a risk factor for aneurysmal rupture or not, but, in general, increased plasma volumes and pregnancy-induced hypertention account for an increased risk of aneurysmal rupture [16].

An early and precise diagnosis is critical, and it is highly recommended to perform CT or MRI on these patients. In general, CT is the first choice to detect hemorrhage, and then MRI follows. Sometimes MRI may be the first method of choice, when exposure to radiation represents an issue. In such cases, fluid-attenuated inversion recovery (FLAIR) is useful for the detection of SAH, which would fail to be detected otherwise [19]. MR angiography is also important to

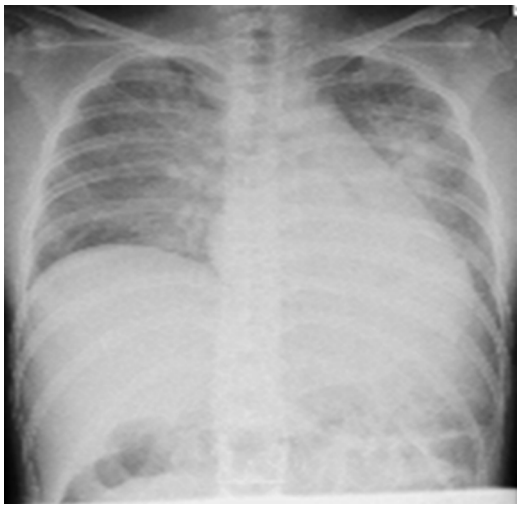

Fig. 4. Chest radiograph of acute pulmonary edema in a woman presenting dyspnea at 26 gestational weeks. The patient was prescribed with ritodrine hydrochloride and magnesium sulfate on the basis of cervical incompetency. The chest radiograph demonstrated enlargement of the cardiac silhouette, bat wing edema with central distribution, and spare of the lung cortex. These features completely disappeared following volume control therapy.

determine the underlying causes of the hemorrhage, e.g. aneurysm, Moyamoya disease, or arterio-venous malformation, without the use of contrast material.

3.2. Lung edema

In comparison with non-pregnant women, healthy pregnant women may present predisposing factors to lung edema, such as hyperdynamic circulation, physiological anemia and low colloid osmotic pressure. The incidence of acute pulmonary edema is estimated at 0.8:1000 pregnancies, with significant maternal mortality. It occurs most commonly in the antepartum period, closely followed by the postpartum period. The common causes are the use of tocolytic agents, especially when multiple tocolytics are used simultaneously (Fig. 4), cardiac diseases including peripartum cardiomyopathy, iatrogenic fluid overload, and preeclampsia. In such cases, chest radiograph is mandatory and typical features including upper lobe redistribution, pulmonary infiltrates, and Kerley-B lines should be sought [17]. Transthoracic endocardiography is the primary diagnostic and management tool [17].

Keeping this disease and pregnancy-specific causes in mind allows for immediate management, avoiding unnecessary examinations such as CT [20].

4. Hormonal changes

To develop and maintain an environment favorable to pregnancy and to fetal growth, significant hormonal changes take place. The placenta plays an important role in the large-scale production of a wide variety of pregnancy-related hormones, such as human chorionic gonadotropin (hCG), estrogen, and progesterone. These hormonal changes alter the endocrine system, which may in turn lead to unexpected complications.

4.1. Hyperemesis and Wernicke encephalopathy

Hyperemesis is defined as a severe vomiting disorder resulting in weight loss, dehydration, alkalosis due to the loss of hydrochloric acid, and hypokalemia. It is related to high or rapidly rising serum levels of pregnancy-related hormones.

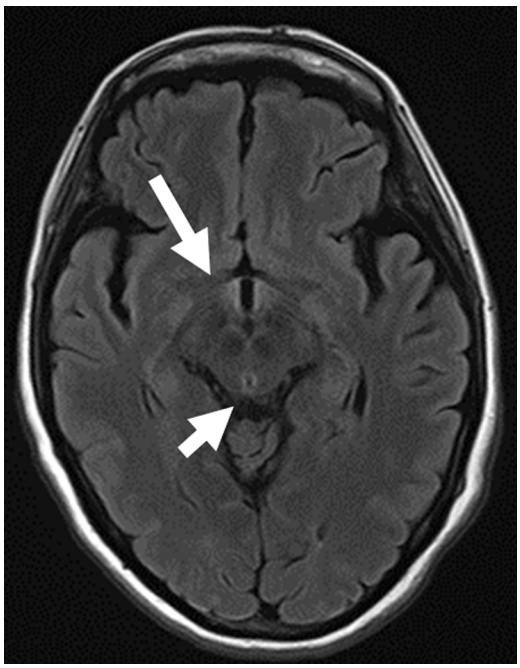

Fig. 5. MRI scan of Wernicke's encephalopathy in a non-pregnant woman presenting alcohol addiction. Axial fluid-attenuated inversion recovery (FLAIR) images showed symmetrical hyperintense signals around the third ventricle (long arrow) and the aqueduct of the midbrain (short arrow).

Wernicke's encephalopathy (WE) is a rare but known complication of severe hyperemesis gravidarum caused by vitamin B1 deficiency. The body's stored amount of vitamin B1 may be depleted in only 3 weeks. WE is a potentially fatal medical emergency and may result in spontaneous fetal loss [21]. Wernicke's classic triad (i.e., confusion, ocular abnormalities and ataxia), is only part of a wider variety of features, thus, WE should be suspected whenever a pregnant patient with persistent vomiting, develops neurologic alterations [21].

The diagnosis is confirmed on clinical manifestations and rapid reversal of symptoms with thiamine. MRI allows for a rapid diagnostic confirmation with high specificity (93%) and moderate sensitivity (53%) [22]. Typical imaging features include symmetrical high intensity in the mesencephalic tegmentum, mammillary bodies, and medial thalamus on T2-weighted images (T2WI) and FLAIR (Fig. 5). DWI may also depict lesions and allows the distinction between vasogenic and cytotoxic edema, which is important to make a prognosis [21].

4.2. Pituitary apoplexy

Pituitary apoplexy is an acute syndrome characterized by symptoms such as headache, visual deficits, and ophthalmoplegia associated with an acutely enlarging adenoma caused by hemorrhage or infarction. Its incidence increases during pregnancy and post-partum period, which might be explained by the increased pituitary stimulation from placental estrogens, the enlargement of the adenohypophysis, or the rapid growth of tumors, and may also result from ischemia [23].

On CT, a heterogeneous sellar/suprasellar mass may be seen along with hemorrhagic apoplexy, appearing as a dense mass in the acute phase. MRI depicts an enlarged pituitary with variable T1 and T2 signal intensities, depending on the age of the hemorrhage (Fig. 6). An apoplexy secondary to infarction may also be detected earlier using DWI [16,24].

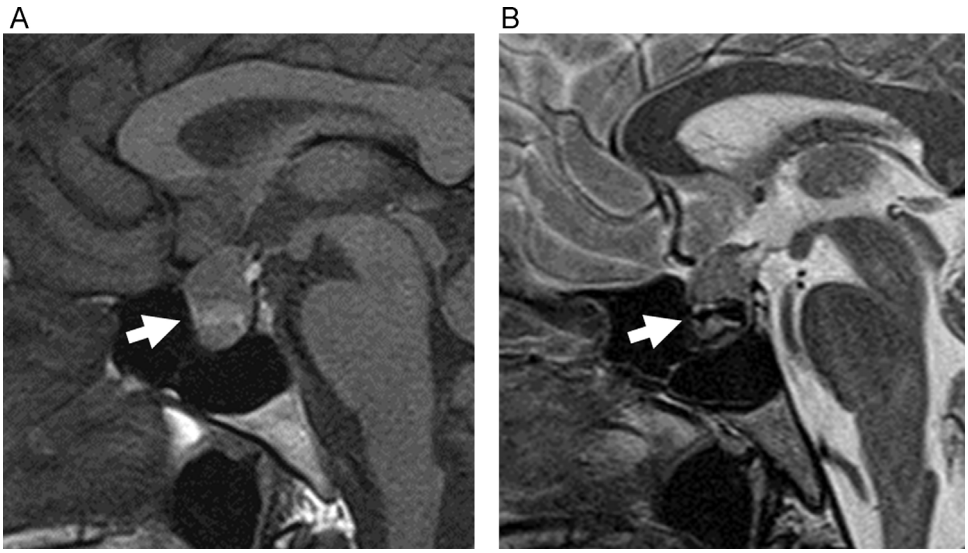

Fig. 6. MRI scan of pituitary hemorrhagic apoplexy in a woman presenting prolactinoma at 34 gestational weeks. The patient also presented symptoms of headache and vomiting. An enlarged pituitary gland was observed with focal hemorrhage, high signal intensity on sagittal T1-weighted image (A: arrow) and low signal intensity on sagittal T2-weighted image (B: arrow).

4.3. Gallstones and complications

Gallstones and cholecystitis are the second most common non-obstetric emergency requiring surgery in pregnant patients, after acute appendicitis [4]. During a normal pregnancy, high levels of estrogen and progesterone may impair gallbladder motility function, which increase the incidence of gallstones by up to 12% [25]. Although the incidence of cholecystitis does not increase in normal pregnancy, the incidences of both gallstones and cholecystitis increase among patients with intrahepatic cholestasis of pregnancy, a rare pregnancy-specific liver condition. Intrahepatic cholestasis of pregnancy is a disorder characterized by pruritus, elevated serum aminotransferases and bile acid levels with onset in the second or the third trimester of pregnancy, and a spontaneous relief occurs within 2–3 weeks after delivery [26].

Ultrasonography is the imaging modality of choice due to its high sensitivity and specificity, however, ultrasonography may be limited by the patient's body habitus, especially in obese patients. MR cholangiopancreatography (MRCP) is the most appropriate second-line imaging method, as it is highly sensitive and specific for the detection of biliary disease and more sensitive than ultrasonography for the detection of choledocholithiasis [4,25]. The stones appear indeed as a filling defect within the high signal bile region.

5. Mechanical pressure exerted by an enlarged uterus

During pregnancy, the enlarging uterus leads to the compression and displacement of other organs. This may thus increase the risk of specific complications and sometimes make diagnosis more intricate than in non-pregnant patient cases.

5.1. Acute appendicitis

Acute appendicitis is the most common non-obstetric emergency requiring surgery during pregnancy. The incidence is estimated at 1:1700 pregnancies [4], the same as in the non-gravid population.

The diagnosis of acute appendicitis is challenging in the pregnant patient because the typical symptoms and clinical findings may also be present in a normal pregnancy. The displacement of the appendix by the enlarging uterus also makes the diagnosis difficult. Appendiceal rupture is more frequent in pregnant women, possibly due to the delay in diagnosis and treatment [27], and the rupture is highly associated with perinatal mortality. Prompt and accurate diagnosis is therefore critical.

Ultrasonography is classically the first imaging method employed, however, there are limitations including high rates of indeterminate examinations and dependency on the operator. In those cases, CT or MRI should be performed. MRI is now a well-established imaging tool for appendicitis in pregnancy with high sensitivity and specificity [28]. CT and MRI findings will classically show an appendiceal diameter greater than 7 mm, increased wall thickness, fluid collection in the appendix and periappendiceal fat inflammation (Fig. 7) [11,29]. Multiplanar assessments with rapid sequences such as T2-weighted single-shot fast spin-echo (SSFSE) images (Fig. 7) and T2WI with fat suppression for detection of periappendiceal inflammation are recommended [28].

5.2. Urological disease

Mechanical compression from the enlarged gravid uterus and smooth muscle relaxation induced by progesterone may lead to urinary stasis [30]. Altogether, the risk of pyelonephritis is increased during pregnancy (1–2%) [30,31]. The susceptibility of pregnant women to urinary tract infection should be kept in mind.

In relation to maternal hydronephrosis, a physiologic hydronephrosis remains the most common, which may mimic a pathologic hydronephrosis. It occurs in 60–94% of pregnant women, usually late in pregnancy, due to ureteral compression by the gravid uterus, with predominant incidence in the right flank (80–90%) [4,29]. A physiologic hydronephrosis is characterized by the smooth tapering of the ureter at the level of the sacral promontory, without pathological causes of obstruction (Fig. 8). On the other hand, a pathologic hydronephrosis classically presents a site of obstruction at the pelvoureteral or vesicoureteral junction, and an abrupt ending of the hydroureter (Fig. 9) [32]. The most common cause of hydronephrosis during pregnancy is a stone and the incidence of symptomatic cases is estimated to be 0.5:1000 pregnancies, similar to that of non-pregnant women, with equal incidence in the right and left flanks [32,33].

The role of imaging is to make the distinction between physiologic and pathologic hydronephrosis. Again, ultrasonography is the

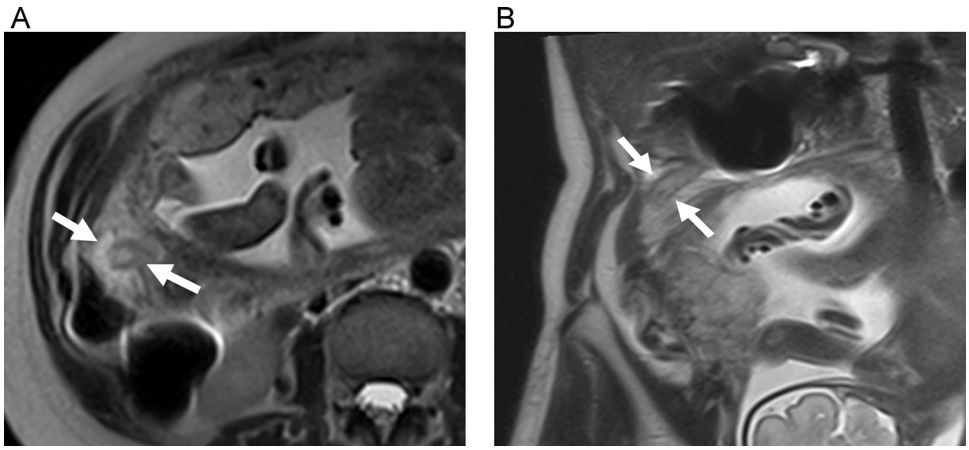

Fig. 7. MRI scan of acute appendicitis in a woman with right abdominal pain at 28 gestational weeks. Axial (A: arrow) and coronal (B: arrow) single shot first spin echo (SSFSE) images demonstrated fluid collection in the dilated appendix (9 mm), located at the level of the inferior margin of the liver.

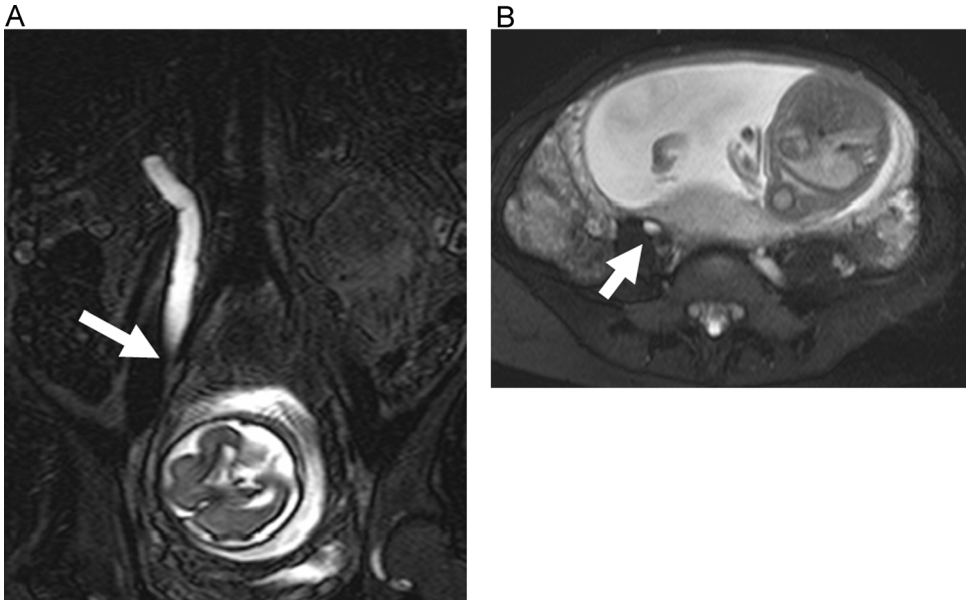

Fig. 8. MRI scan of physiologic hydronephrosis in a woman presenting right flank pain at 25 weeks of gestation. Right hydronephrosis and hydroureter were observed (A: arrow). A dilated right ureter tapered gradually to the level of the sacral promontory (B: arrow). (A) Coronal single-shot T2-weighted image with breath hold and fat suppression and (B) axial T2-weighted image with fat suppression.

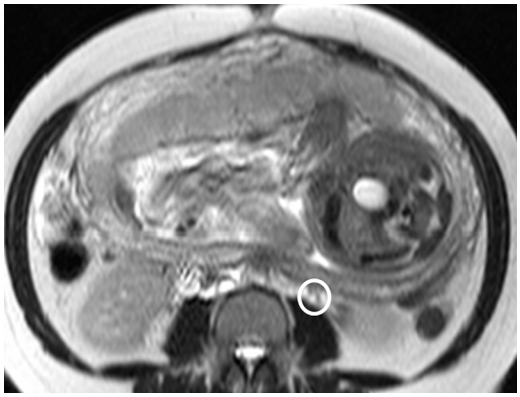

Fig. 9. MRI scan of pathologic hydronephrosis in a woman presenting left flank pain at 29 weeks of gestation, and clinically diagnosed with ureteral lithiasis. Left hydronephrosis and hydroureter at the level of lumbars 3–4 (circle) were observed on axial T2-weighted images. The unusual side and site of obstruction suggested a case of pathologic hydronephrosis.

first-line modality, but does not allow depicting the entire ureter, and the obstructed site often fails to be observed. Transvaginal ultrasonography is effective to detect stones at the ureterovesical junction [4]. Unenhanced CT is often the second-line imaging modality, as it offers high sensitivity in the detection of ureteral stones, nearing 100%. The implementation of reduced radiation dose CT protocols may be adopted without compromising the accuracy [4]. Alternatively, MR urography is also a useful imaging tool during pregnancy, as it was reported to show dilated ureter, obstructed site, and allowed identification of the cause of the obstruction, thus eliminating exposure to radiation [11,33]. The sensitivity and specificity of MR urography in diagnosing ureteral stones are 77% and 83%, respectively. On MR urography and T2WI, ureteral stones are depicted as ureteral filling defects. Care should be taken not to mistake blood, proteins in urine, flow artifact, ureteral air, or surgical clips for a stone [4,32]. In a patient with acute obstruction, perirenal and periureteral high intensity may be observed on T2WI, which are absent in patients with chronic obstruction or physiologic hydronephrosis [11]. MRI also represents a helpful tool to demonstrate complications, such

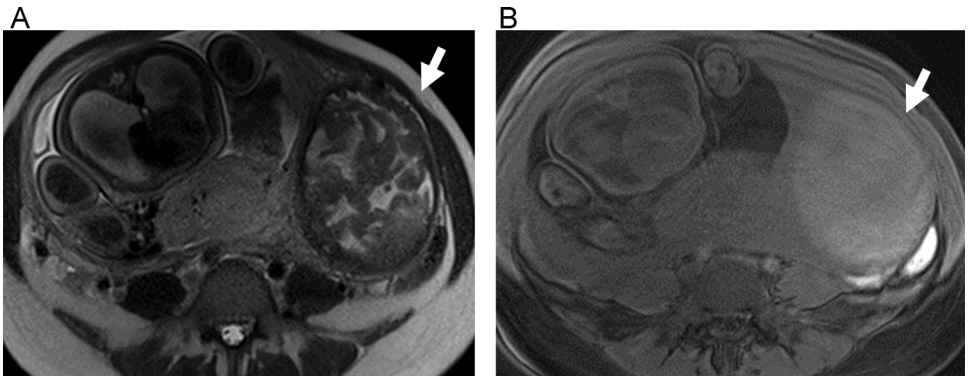

Fig. 10. MRI scan of red degeneration of uterine leiomyoma in a pregnant woman at 36 weeks of gestation. The leiomyoma showed a heterogenous signal intensity with a hypointense rim on T2-weighed images (A) and mildly hyperintense signals on T1-weighted images with fat suppression (B).

as pyelonephritis, which is visualized as an enlarged edematous kidney [32].

5.3. Red degeneration of uterine leiomyoma

During pregnancy, uterine leiomyomas will likely undergo red degeneration, also known as hemorrhagic infarction, at a rate of 8% [34]. It results from the enlargement of the uterus, leading to alteration of blood supply and ischemia of leiomyomas [29]. Clinical findings include severe localized abdominal pain, tenderness on palpation, and sometimes low-grade fever and leukocytosis. The condition is often difficult to distinguish from other complications such as appendicitis. An accurate diagnosis is important, because a conservative management is recommended in such cases. MRI should be the primary diagnostic tool used, and classical features include visualization of the rim characteristic of degenerated leiomyomas, hyper-intense signals on T1WI and hypo-intense signals on T2WI (Fig. 10) [34].

5.4. Ovarian torsion

Ovarian torsion is defined as the partial or complete rotation of the ovary and its vascular pedicle on the suspensory ligament, with a right-sided predominance [35]. The incidence rises during pregnancy (1:1800), especially in the first trimester, when the uterus undergoes a rapid increase in size. The most common cause during pregnancy is a corpus luteum cyst. Torsion of normal ovary may also be more common in pregnant women than in non-pregnant women, owing to ligamentous laxity.

Because tissue necrosis can occur rapidly, a prompt diagnosis and treatment are essential to preserve ovarian functions and healthy pregnancy. Ultrasonography is the first-line imaging modality and its features of ovarian torsion include enlarged adnexal structures and peripheral ovarian lesions [35]. CT and MRI may also be performed for confirmation or differentiation of the diagnosis. MRI is considered to be more appropriate than CT during pregnancy, as this eliminates patient exposure to radiation. CT and MRI features include ovarian enlargement (>4.0 cm) with or without mass, subacute hemorrhage, twisted pedicle, deviation of the uterus to the affected side, engorged vessels, and fallopian tube thickening [35]. On MRI, the enlarged edematous ovary and its peripheral follicles are clearly observed on T2WI (Fig. 11). On T1WI with fat saturation, subacute hemorrhage is characterized by the presence of a hyperintense rim. Multiplanar CT reformations or MRI acquisitions are optimal for detection of a twisted pedicle, the pathognomonic finding of ovarian torsion [35].

6. Preeclampsia, eclampsia and HELLP syndrome

Preeclampsia, eclampsia, and HELLP syndrome are multisystemic disorders sharing pathogenic, pathologic and clinical features and result from systemic vascular endothelial damage and

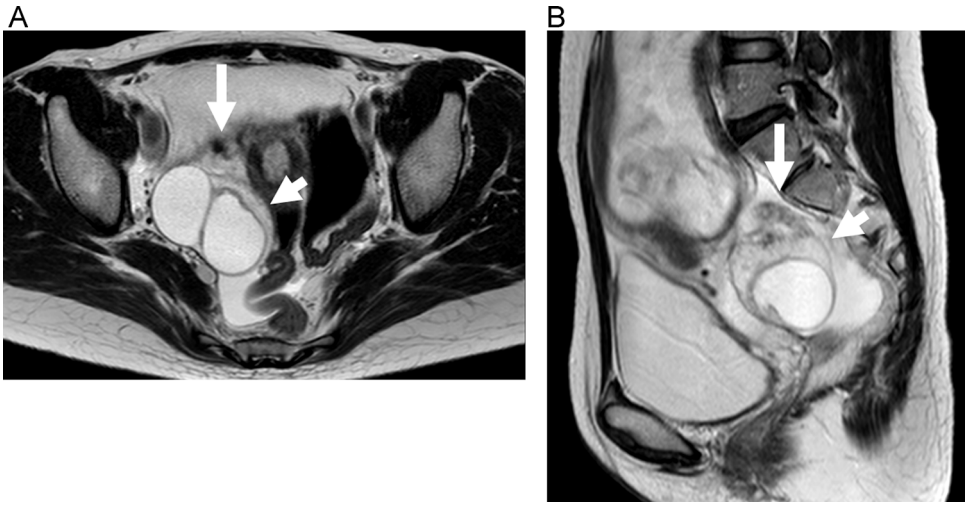

Fig. 11. MRI scan showing torsion of the right ovary with a corpus luteum cyst in a woman at 15 gestational weeks. The markedly edematous ovarian parenchyma (A and B: short arrow) and twisted pedicle (A and B: long arrow) were visible. Multiplanar assessments are optimal for the detection of such findings. (A) Axial T2-weighted image and (B) sagittal T2-weighted image.

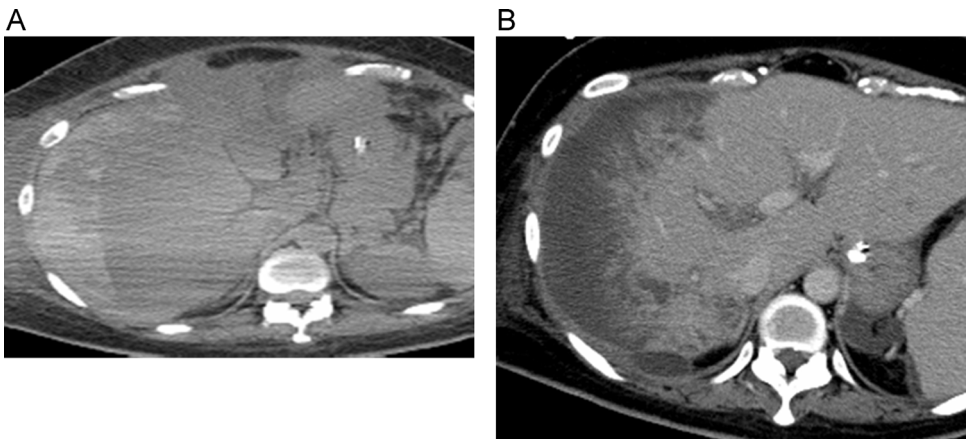

Fig. 12. A woman with preeclampsia developed HELLP syndrome and hepatic subcapsular hemorrhage 2 days after an emergency cesarean section. A hematoma appeared as a high density lesion in the subcapsular space on plain CT (A). Streak artifacts due to the arms-down position were visible. Contrast enhanced CT scan (B) obtained 2 weeks after delivery revealed liver infarction in the peripheral zone of the right lobe and decreased density of the subcapsular hematoma.

vasospasm [36]. Diagnosis of these diseases is based on both clinical and biochemical criteria. The role of imaging is to diagnose the associated complications and their severity.

Preeclampsia is clinically defined by hypertension and proteinuria, with or without pathologic edema. Eclampsia is defined by the onset of convulsions in a woman with preeclampsia that cannot be attributed to other causes. HELLP syndrome is clinically described as the combined occurrence of hemolysis, elevated liver enzyme levels, and low platelet levels during pregnancy. It is associated with a high maternal death rate and important perinatal mortality. It is believed that vasospasms are the causes of endothelial damage and fibrin deposition, followed by accelerated platelet aggregation and consumption thrombocytopenia, thrombotic microangiopathy, and hemolytic anemia [36]. It is typically complicated by severe preeclampsia or eclampsia but can also occur independently [36]. The incidence is approximately 0.1–0.6% of pregnancies, and 4–12% of patients with severe eclampsia [37]. In many cases (70%), the condition is diagnosed antepartum, with 90% of them made after 27 weeks of gestational age. However, it should be kept in mind that the remaining 30% are diagnosed postpartum [36].

The common complications associated with the above disorders include hemorrhagic stroke, disseminated intravascular coagulation, acute renal failure, lung edema, hepatic disorders, placental disorders, posterior reversible encephalopathy syndrome (PRES), and so on. Here, we put the emphasis on hepatic disorders and PRES.

6.1. Hepatic disorders associated with HELLP syndrome and preeclampsia

A diseased liver is often associated with devastating consequences, especially in HELLP syndrome. The hepatic pathology of HELLP syndrome includes focal hepatocyte necrosis, periportal hemorrhage and fibrin deposits in the hepatic sinusoids [36]. In more severe cases, complications such as liver hemorrhage and infarction may also occur. Acute fatty liver of pregnancy (AFLP) has also been associated with preeclampsia and HELLP syndrome.

6.2. Acute fatty liver of pregnancy

AFLP is a rare, but, serious complication usually occurring in the third trimester of nulliparous patients, with an incidence of 0.7–1.0:10,000 pregnancies [38]. Approximately half of the patients with AFLP present preeclampsia [39].

AFLP is characterized by microvesicular fatty infiltration of hepatocytes without any inflammation or necrosis, leading to eventual coagulopathy and hypoglycemia secondary to hepatic failure [38]. AFLP may result in significant perinatal and maternal mortality. Early diagnosis with immediate termination of pregnancy and intensive supportive care is essential. Recovery is usually complete, even after severe hepatic dysfunction.

The diagnostic criteria do not include imaging findings and the main role of imaging is to exclude other diseases [19]. Ultrasonography might be the first-line imaging modality, however, its sensitivity is low, and the characteristic diffuse increase of hepatic parenchymal echogenicity is only detected in 20–27% of the examined patients. Unenhanced CT shows hypo-attenuation of the hepatic parenchyma in 20–50% of the patients [28]. MRI is the most sensitive modality for the detection of cytoplasmic lipids. The signal dropout is classically observed on opposed-phased T1WI. MRI may be a useful alternative to liver biopsy, which is not recommended in the current management, due to a high incidence of coagulopathies in women with AFLP [40].

6.3. Liver hemorrhage and infarction

Liver hemorrhage and infarction are rare, but severe and devastating complications of HELLP syndrome. They can also complicate the pathology of preeclampsia/eclampsia.

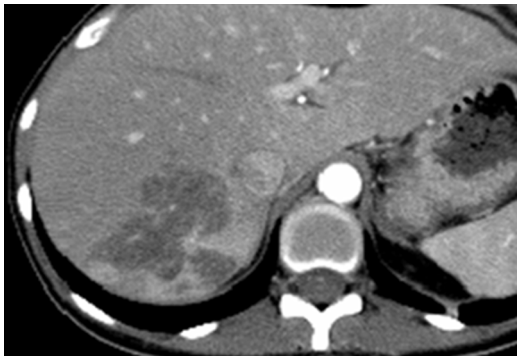

Fig. 13. A woman presenting preeclampsia developed intracerebral hemorrhage and liver infarction, 6 days after an emergency cesarean section. Contrast-enhanced CT showed a poorly enhanced geographic area with coursing enhanced vessels in the posterior segment of the liver.

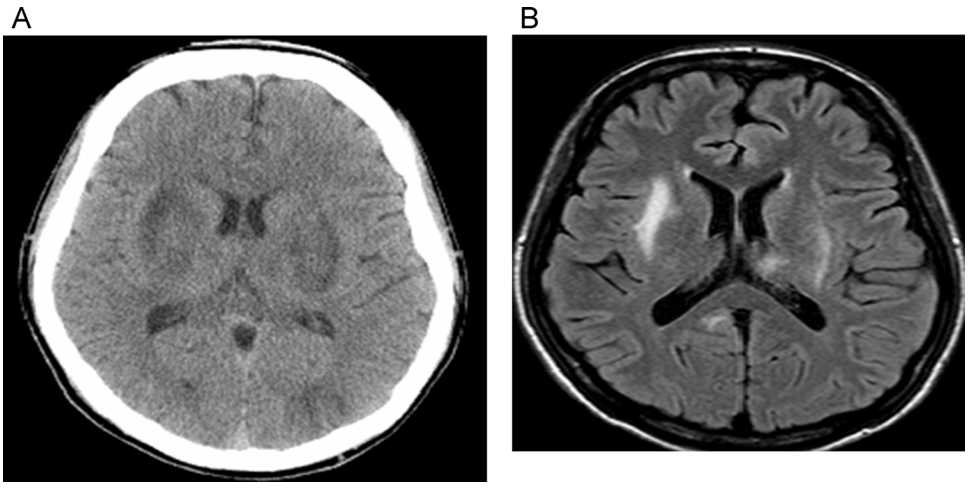

Fig. 14. Posterior reversible encephalopathy syndrome (PRES) in a woman presenting eclampsia and HELLP syndrome at 28 weeks of gestation. (A) CT scan at the onset eclampsia showing multiple low signal density areas including the bilateral putamen, external capsule, thalami and left occipital lobe. The pons was also involved. (B) Fluid-attenuated inversion recovery (FLAIR) images showing multiple hyperintense regions/spots, which completely disappeared in the follow-up images taken 1 month after treatment.

Imaging findings of hemorrhage vary depending on the age of the blood products but are typically manifested as a heterogeneous, space-occupying peripheral lesion in the parenchyma or the subcapsular space [25]. Although ultrasonography can be performed rapidly without radiation exposure, CT facilitates the characterization of hematomas and precise determination of the site and extent of the intraperitoneal hemorrhage (Fig. 12). CECT shows the intraparenchymal hepatic hematomas to be lower in attenuation than the adjacent liver. When hepatic rupture occurs, CT will show a site of focal irregularity with an adjacent sentinel clot or findings of remote hemoperitoneum [25].

Imaging findings of infarction include peripheral geographic bands of hypoechogenicity upon ultrasonography and decreased attenuation upon CT. CECT shows heterogeneous areas of hypoattenuation in a peripheral wedge-shaped pattern, or in a geographic pattern when the lesions are larger, with enhanced vessels coursing through these areas (Fig. 13). In MRI, the corresponding areas are depicted as mildly high intensity on T2WI and low intensity on T1WI [25].

6.4. *Posterior reversible encephalopathy syndrome (PRES)*

PRES is a clinically recognizable entity presenting features such as headache, altered consciousness, visual abnormalities, and seizures in conjunction with the neuroimaging findings of vasogenic edema, typically involving the posterior circulation. This condition is likely induced by endothelial dysfunction leading to increased permeability [16]. Several studies have shown that neurological imaging findings consistent with PRES were present in many patients with severe preeclampsia/eclampsia [41–43].

A typical MRI finding associated with PRES is hyperintensity of the parieto-occipital cortices and subcortical white matter on T2WI and FLAIR images, usually indicating vasogenic edema (Fig. 14B). The posterior frontal and inferior temporal regions, and less commonly the brainstem, basal ganglia, and cerebellum, are involved. The lesions rarely demonstrate contrast enhancement, hemorrhage, or restricted diffusion. Unenhanced CT might be performed at first to exclude hemorrhagic stroke. The lesions are classically depicted as low density area (Fig. 14A) [16]. Less severe edema, cytotoxic edema, hemorrhage, and contrast enhancement have been reported. In follow-up MRI, more frequent complete resolutions of edema were observed [44].

7. Conclusion

The dynamic changes occurring during pregnancy may induce a variety of non-obstetric complications affecting organs from head to toe. A deep understanding of the imaging findings associated with these various conditions and their pathophysiological relevance to pregnancy will allow a more precise and early diagnosis, ensued by an early treatment.

Conflict of interest

The authors have nothing to disclose.

Acknowledgement

We thank Kazushige Tsutsui, Department of Radiology, Japanese Red Cross Society Wakayama Medical Center, Wakayama, Japan, for assistance in preparing the manuscript.

References

[1] P.E. Marik, Venous thromboembolism in pregnancy, Clin. Chest Med. 31 (4) (2010) 731–740.
[2] P.E. Marik, L.A. Plante, Venous thromboembolic disease and pregnancy, N. Engl. J. Med. 359 (19) (2008) 2025–2033.
[3] M.A. Miller, M. Chalhoub, G. Bourjeily, Peripartum pulmonary embolism, Clin. Chest Med. 32 (1) (2011) 147–164, ix–x.
[4] P.I. Wang, S.T. Chong, A.Z. Kielar, et al., Imaging of pregnant and lactating patients. Part 2. Evidence-based review and recommendations, AJR Am. J. Roentgenol. 198 (4) (2012) 785–792.
[5] G. Bourjeily, M. Paidas, H. Khalil, K. Rosene-Montella, M. Rodger, Pulmonary embolism in pregnancy, Lancet 375 (9713) (2010) 500–512.
[6] M.A. Kominiarek, J.U. Hibbard, Postpartum ovarian vein thrombosis: an update, Obstet. Gynecol. Surv. 61 (5) (2006) 337–342.
[7] C.E. Brown, R.W. Stettler, D. Twickler, F.G. Cunningham, Puerperal septic pelvic thrombophlebitis: incidence and response to heparin therapy, Am. J. Obstet. Gynecol. 181 (1) (1999) 143–148.
[8] P.J. Woodward, A. Kennedy, R. Sohaey, Postpartum complications, in: Diagnostic Imaging Obstetrics, Amirsys, 2011.
[9] D.M. Twickler, A.T. Setiawan, R.S. Evans, et al., Imaging of puerperal septic thrombophlebitis: prospective comparison of MR imaging, CT, and sonography, AJR Am. J. Roentgenol. 169 (4) (1997) 1039–1043.
[10] R.A. Kubik-Huch, G. Hebisch, R. Huch, P. Hilfiker, J.F. Debatin, G.P. Krestin, Role of duplex color Doppler ultrasound, computed tomography, and MR angiography in the diagnosis of septic puerperal ovarian vein thrombosis, Abdom. Imaging 24 (1) (1999) 85–91.
[11] M. Nagayama, Y. Watanabe, A. Okumura, Y. Amoh, S. Nakashita, Y. Dodo, Fast MR imaging in obstetrics, Radiographics 22 (3) (2002) 563–580, discussion 80–82.

[12] J.R. Leyendecker, V. Gorengaut, J.J. Brown, MR imaging of maternal diseases of the abdomen and pelvis during pregnancy and the immediate postpartum period, Radiographics 24 (5) (2004) 1301–1316.
[13] C. Jaigobin, F.L. Silver, Stroke and pregnancy, Stroke 31 (12) (2000) 2948–2951.
[14] L. Foo, S. Bewley, A. Rudd, Maternal death from stroke: a thirty year national retrospective review, Eur. J. Obstet. Gynecol. Reprod. Biol. 171 (2) (2013) 266–270.
[15] A.H. James, C.D. Bushnell, M.G. Jamison, E.R. Myers, Incidence and risk factors for stroke in pregnancy and the puerperium, Obstet. Gynecol. 106 (3) (2005) 509–516.
[16] A.M. Mortimer, M.D. Bradley, M. Likeman, N.G. Stoodley, S.A. Renowden, Cranial neuroimaging in pregnancy and the post-partum period, Clin. Radiol. 68 (5) (2013) 500–508.
[17] A.T. Dennis, C.B. Solnordal, Acute pulmonary oedema in pregnant women, Anaesthesia 67 (6) (2012) 646–659.
[18] C.A. Scott, S. Bewley, A. Rudd, et al., Incidence, risk factors, management, and outcomes of stroke in pregnancy, Obstet. Gynecol. 120 (2 Pt 1) (2012) 318–324.
[19] M. Mohamed, D.C. Heasly, B. Yagmurlu, D.M. Yousem, Fluid-attenuated inversion recovery MR imaging and subarachnoid hemorrhage: not a panacea, AJNR Am. J. Neuroradiol. 25 (4) (2004) 545–550.
[20] A. Sciscione, Acute pulmonary edema in pregnancy, Obstet. Gynecol. 101 (3) (2003) 511–515.
[21] G. Chiossi, I. Neri, M. Cavazzuti, G. Basso, F. Facchinetti, Hyperemesis gravidarum complicated by Wernicke encephalopathy: background, case report, and review of the literature, Obstet. Gynecol. Surv. 61 (4) (2006) 255–268.
[22] E. Antunez, R. Estruch, C. Cardenal, J.M. Nicolas, J. Fernandez-Sola, A. Urbano-Marquez, Usefulness of CT and MR imaging in the diagnosis of acute Wernicke's encephalopathy, AJR Am. J. Roentgenol. 171 (4) (1998) 1131–1137.
[23] P.L. Semple, J.A. Jane Jr., E.R. Laws Jr., Clinical relevance of precipitating factors in pituitary apoplexy, Neurosurgery 61 (5) (2007) 956–961, discussion 61–62.
[24] J.M. Rogg, G.A. Tung, G. Anderson, S. Cortez, Pituitary apoplexy: early detection with diffusion-weighted MR imaging, AJNR Am. J. Neuroradiol. 23 (7) (2002) 1240–1245.
[25] M.T. Heller, M.E. Tublin, K. Hosseinzadeh, A. Fargiano, Imaging of hepatobiliary disorders complicating pregnancy, AJR Am. J. Roentgenol. 197 (3) (2011) W528–W536.
[26] A. Ropponen, R. Sund, S. Riikonen, O. Ylikorkala, K. Aittomaki, Intrahepatic cholestasis of pregnancy as an indicator of liver and biliary diseases: a population-based study, Hepatology 43 (4) (2006) 723–728.
[27] A.B. Weingold, Appendicitis in pregnancy, Clin. Obstet. Gynecol. 26 (4) (1983) 801–809.
[28] P.J. Woodward, A. Kennedy, R. Sohaey, Maternal conditions in pregnancy, in: Diagnostic Imaging Obstetrics, Amirsys, 2011, pp. 1–49.
[29] L.B. Spalluto, C.A. Woodfield, C.M. DeBenedectis, E. Lazarus, MR imaging evaluation of abdominal pain during pregnancy: appendicitis and other nonobstetric causes, Radiographics 32 (2) (2012) 317–334.
[30] F. Smaill, J.C. Vazquez, Antibiotics for asymptomatic bacteriuria in pregnancy, Cochrane Database Syst. Rev. 2 (2007) CD000490.
[31] J.B. Hill, J.S. Sheffield, D.D. McIntire, G.D. Wendel Jr., Acute pyelonephritis in pregnancy, Obstet. Gynecol. 105 (1) (2005) 18–23.
[32] G. Masselli, M. Derme, F. Laghi, et al., Imaging of stone disease in pregnancy, Abdom. Imaging 38 (6) (2013) 1409–1414.
[33] A. Thabet, S.P. Kalva, B. Liu, P.R. Mueller, S.I. Lee, Interventional radiology in pregnancy complications: indications, technique, and methods for minimizing radiation exposure, Radiographics 32 (1) (2012) 255–274.
[34] S. Kawakami, K. Togashi, I. Konishi, et al., Red degeneration of uterine leiomyoma: MR appearance, J. Comput. Assist. Tomogr. 18 (6) (1994) 925–928.
[35] S. Duigenan, E. Oliva, S.I. Lee, Ovarian torsion: diagnostic features on CT and MRI with pathologic correlation, AJR Am. J. Roentgenol. 198 (2) (2012) W122–W131.
[36] D. Mihu, N. Costin, C.M. Mihu, A. Seicean, R. Ciortea, HELLP syndrome – a multisystemic disorder, J. Gastrointest. Liver Dis. JGLD 16 (4) (2007) 419–424.
[37] T.A. Knox, L.B. Olans, Liver disease in pregnancy, N. Engl. J. Med. 335 (8) (1996) 569–576.
[38] H. Ko, E.M. Yoshida, Acute fatty liver of pregnancy, Can. J. Gastroenterol. 20 (1) (2006) 25–30.
[39] E.M. Ong, J.S. Drukteinis, H.E. Peters, K.J. Mortele, Multimodality imaging of hepato-biliary disorders in pregnancy: a pictorial essay, Emerg. Radiol. 16 (5) (2009) 357–363.
[40] A.G. Rajasri, R. Srestha, J. Mitchell, Acute fatty liver of pregnancy (AFLP) – an overview, J. Obstet. Gynaecol. 27 (3) (2007) 237–240.
[41] H. Matsuda, K. Sakaguchi, T. Shibasaki, et al., Cerebral edema on MRI in severe preeclamptic women developing eclampsia, J. Perinat. Med. 33 (3) (2005) 199–205.
[42] O. Demirtas, F. Gelal, B.D. Vidinli, L.O. Demirtas, E. Uluc, A. Baloglu, Cranial MR imaging with clinical correlation in preeclampsia and eclampsia, Diagn. Interv. Radiol. 11 (4) (2005) 189–194.
[43] R.B. Schwartz, S.K. Feske, J.F. Polak, et al., Preeclampsia-eclampsia: clinical and neuroradiographic correlates and insights into the pathogenesis of hypertensive encephalopathy, Radiology 217 (2) (2000) 371–376.
[44] T.G. Liman, G. Bohner, P.U. Heuschmann, M. Scheel, M. Endres, E. Siebert, Clinical and radiological differences in posterior reversible encephalopathy syndrome between patients with preeclampsia-eclampsia and other predisposing diseases, Eur. J. Neurol. 19 (7) (2012) 935–943.